Monitoring of laminated composites delamination based on electro-mechanical impedance measurement

Christophe Bois, Christian Hochard

Monitoring of Laminated Composites Delamination Based on Electro-mechanical Impedance Measurement

CHRISTOPHE BOIS* AND CHRISTIAN HOCHARD

Laboratoire de Mécanique et d'Acoustique, CNRS, 31, Chemin Joseph Aiguier, 13402 Marseille cedex 20, France

ABSTRACT: This paper paves the way for a multi damage monitoring system for composite structures. The final goal of this work being to design a monitoring system able to predict the damage in the composite structure under static and fatigue loading. This system will be based on the simultaneous use of measurement and damage predicting models. We describe the first step of this work, which consists in the use of electro mechanical impedance measurement to detect delamination. An electro mechanical model of a beam into which delamination has been introduced is presented and compared with experimental results. The influence of geometrical parameters is studied and future improvements of our method are outlined.

Key Words: monitoring, composite material, delamination, impedance, piezoelectric

INTRODUCTION

METALLIC structure monitoring has proved to be able to reduce both the risks of accident and maintenance costs. Contrary to monitoring systems adapted to metallic materials and mechanical systems, those designed for composite structures are not yet reliable because their damage mechanisms are multiple. Damage mechanisms of composite structures are complex, so we cannot predict their evolution through measurement only. On the other hand, a predictive model, which takes into account all the mechanical phenomena, is not sufficient because of the uncertainties linked to loading, initial material state and characteristics of the material. Neither measurement nor a model on their own are sufficient to predict the evolution of damage. Therefore a monitoring system for composite materials requires both simulation tools and adapted measurement equipment.

Existing measurement systems generally use piezoelectric transducers in order to measure the damage caused by impacts (Tracy and Chang, 1998). What interests us is not only the damage caused by impacts but also the damage from static and fatigue loading. An ideal system should determine the kind of damage produced, whether it is diffuse damage (micro cracks), cracks or delamination, to locate it and measure its degree (Figure 1). Such a system is not realizable in the near future. Our objective is to differentiate a diffuse damage from a delamination and a laminate fracture, to measure the mean level of diffuse damage in a laminate, to detect a macro-damage and to control its evolution.

*Author to whom correspondence should be addressed.
E-mail: bois@lma.cnrs-mrs.fr

Various methods make it possible to detect the appearance of degradation within a laminate:

- Lamb wave transmission between two transducers (Osmont et al., 2002): Damage is revealed through a change in the wave's propagation velocity and attenuation and through wave diffraction.
- Electrical impedance response of a piezoelectric transducer embedded in the structure (Saint-Pierre et al., 1998). With this method, degradation causes a modification in the dynamic spectrum.

Both measurement methods can be carried out with the same transducers.

The aim is then to predict the evolution of damage from behaviour modelling. Ply scale models based on damage mechanics are able to estimate the level of diffused damage, represented by internal variables, under static and fatigue loading (Ladevèze and Le Dantec, 1992; Payan and Hochard, 2001). By modelling the degradation of the interface, these models can

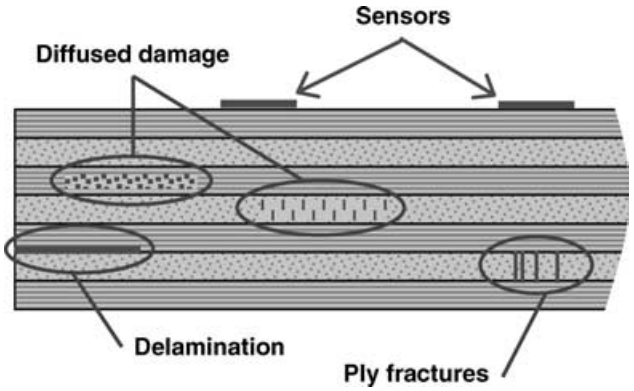

Figure 1. *Damage monitoring of a laminated composite.*

predict the appearance and evolution of delamination (Allix et al., 1998).

This paper focuses on the delamination detection using electro-mechanical impedance measurement. We present here a model of a laminated beam into which we have introduced a delamination and a piezoelectric ply. Simulation and experimental results are then compared. We show a piezoelectric impedance technique which provides information on the size and the position of a delamination which is located inside the beam's structure. Simulations allow us to investigate more closely the influence of some parameters such as damage depth and sensor size which are difficult to modify experimentally. Lastly, we conclude on the way to improve measurement and to extend this method to industrial applications.

ELECTRO-MECHANICAL IMPEDANCE MEASUREMENT

Mechanical impedance, which has been used for several decades in NDC, make it possible to visualize modes on a spectral response. The piezoelectric behaviour couples the mechanical and electrical phenomena. Thus, the electro-mechanical impedance measurement (Figure 2) can give the information contents in mechanical impedance measurement (Giurgiutiu and Rogers, 2000). Saint-Pierre et al. (1998) and Monnier et al. (2000) have successfully used this method to characterise the local properties of polymer materials. They embedded a piezoelectric disc in the material and they compared experimental measurements to one-dimensional simulation in order to extract two acoustical parameters: celerity and attenuation. Our goal is to determine the structural modes modified or created by the presence of delamination. To do that, we compare the experimental results to simulations.

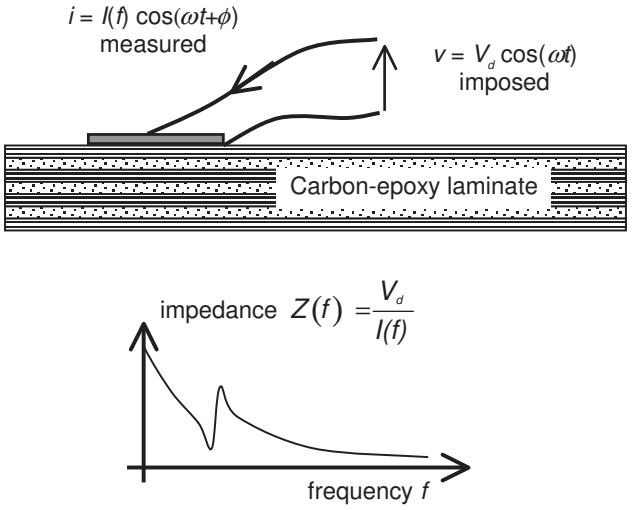

Figure 2. *Electro mechanical impedance measurement.*

ELECTRO-MECHANICAL MODEL OF A COMPOSITE BEAM

To test the feasibility of this method and understand the physical phenomena, we chose beams as our first application. A model allows us to evaluate quickly the influence of various parameters such as the size of the structure, the size and the position of the transducer, the size and the position of the delamination. These results can also facilitate the design of samples.

The model has to take into account the piezoelectric behaviour and simulate the presence of a delamination. Keilers and Chang (1995) dealt with symmetrical beam (delamination in the midplane and transducers on both sides of the laminate). Giurgiutiu and Zagrai (2001) proposed a modelling of a PZT active sensor installed on a structural substrate using the impedance of each element. Our model is based on the laminate theory. Additional electrical assumptions allow us to integrate the piezoelectric constitutive laws in the thickness. Then a delamination is incorporated while respecting the stress continuity.

Description of the Model

Figure 3 defines the parameters of the structure. Its width, in the third direction, is noted b. We divided the beam into 6 sections (Figure 4). Then we used the 3D behaviour relations between the stress tensor $\boldsymbol{\sigma}$ and the displacement vector $\mathbf{u}$ to establish the beam behaviour relations binding the bending moment M, the axial force N, the deflection v and the axial displacement u for each laminate section.

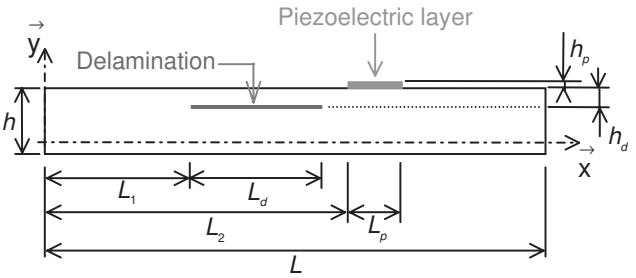

Figure 3. *Structure parameters.*

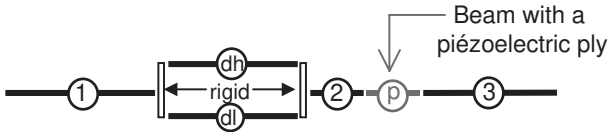

Figure 4. *Beam cutting.*

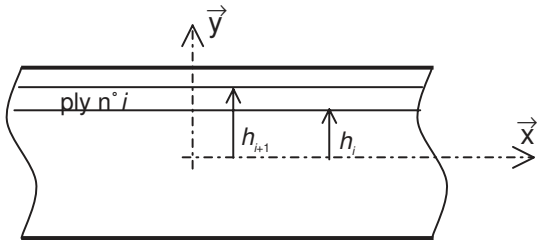

Figure 5. *Laminate description.*

Consider a laminated composite comprising n plies, among which one, subscripted p, has a piezoelectric behaviour (Figure 5). A potential difference V_d is applied between the terminals (+: $y = h_{p+1}$ and –: $y = h_p$) of the piezoelectric ply. Under this electric loading and since the piezoelectric ply is thin, the electric field $\boldsymbol{E}$ has a particular direction: $E = E_2\ y$ and we can assume that $E_2 = V_d/(h_{p+1} - h_p)$.

Use the definition of the bending moment M and the axial force N:

$$M = -b\int_{h_1}^{h_{n+1}} \sigma_{11}(y) y dy \tag{1}$$

$$N = b\int_{h_1}^{h_{n+1}} \sigma_{11}(y) dy \tag{2}$$

The 3D constitutive relations are:

$$\varepsilon_{ij} = S^E_{ijkl}\sigma_{kl} + d_{ijk}E_k \tag{3}$$

$$D_k = d_{kij}\sigma_{ij} + \varepsilon^\sigma_{kl}E_l \tag{4}$$

with:

$$\varepsilon_{ij} = \tfrac{1}{2}\left(u_{i,j} + u_{j,i}\right), \quad E_l = V_{,l} \tag{5}$$

The assumption of Voigt is:

$$\varepsilon_{11} = \gamma y + \varepsilon_0 \tag{6}$$

with:

$$\gamma = -\frac{d^2v}{dx^2}, \qquad \varepsilon_0 = \frac{du}{dx} \tag{7}$$

Then,

$$M = I_3\frac{d^2v}{dx^2} - I_2\frac{du}{dx} + J_2V_d \tag{8}$$

$$N = -I_2\frac{d^2v}{dx^2} + I_1\frac{du}{dx} - J_1V_d \tag{9}$$

$$D = -G\frac{d^2v}{dx^2} + K\frac{du}{dx} + PV_d \tag{10}$$

with:

$$I_q = b\sum_{i=1}^{n} E_i\frac{h^q_{i+1} - h^q_i}{q}, \qquad J_q = -bE_pd_{211}\frac{h^q_{p+1} - h^q_p}{q(h_{p+1} - h_p)},$$
$$G = \frac{d_{211}E_p(h_{p+1} + h_p)}{2}, \qquad K = d_{211}E_p,$$
$$P = \frac{\varepsilon^\sigma_{22} - E_pd^2_{211}}{h_{p+1} - h_p}, \qquad E = \frac{1}{S^E_{1111}} \tag{11}$$

The mechanical equilibrium equations are:

$$\frac{d^2M}{dx^2} + \lambda\frac{d^2v}{dt^2} = 0 \tag{12}$$

$$\frac{dN}{dx} - \lambda\frac{d^2u}{dt^2} = 0 \tag{13}$$

where λ is the linear mass of the beam. Using Equations (8) and (9), we obtain two differential equations in u and v:

$$I_3\frac{d^4v}{dx^4} - I_2\frac{d^3u}{dx^3} + \lambda\frac{d^2v}{dt^2} = 0 \tag{14}$$

$$-I_2\frac{d^3v}{dx^3} + I_1\frac{d^2u}{dx^2} - \lambda\frac{d^2u}{dt^2} = 0 \tag{15}$$

Note that if the laminated composite is symmetrical, we have $I_2 = 0$ and therefore, the two equations are uncoupled. However, in the delaminated zone, or in those zones with a piezoelectric layer, the dissymmetry is inevitable.

We consider the established responses to an excitation $V_d = V_d\ e^{i\omega t}$, i.e., the solutions u and v written as $u = u\,e^{i\omega t}$ and $v = v\ e^{i\omega t}$. Thus, (14) and (15) give:

$$I_3\frac{d^4v}{dx^4} - I_2\frac{d^3u}{dx^3} - \lambda\omega^2v = 0 \tag{16}$$

$$-I_2\frac{d^3v}{dx^3} + I_1\frac{d^2u}{dx^2} + \lambda\omega^2u = 0 \tag{17}$$

We seek the solutions for frequencies close to those of the relatively low frequency bending modes. The angular frequency of the first bending mode is much lower than that of the first axial mode as long as $L/h \ll 1$. Therefore:

$$I_1\frac{d^2u}{dx^2} \gg \lambda\omega^2u \tag{18}$$

and (17) gives:

$$\frac{d^2u}{dx^2} = \frac{I_2}{I_1}\frac{d^3v}{dx^3} \tag{19}$$

upon substitution in (16), we obtain:

$$R\frac{d^4v}{dx^4} - \lambda\omega^2 v = 0 \tag{20}$$

with:

$$R = I_3 - \frac{I_2^2}{I_1} \tag{21}$$

We seek v and u of the form:

$$\begin{aligned} v(x) = {} & A\cos(\Omega x) + B\sin(\Omega x) \\ & + C\cosh(\Omega x) + D\sinh(\Omega x) \end{aligned} \tag{22}$$

$$\begin{aligned} v(x) = {} & \frac{I_2}{I_1}\Omega[A\cos(\Omega x) + B\sin(\Omega x) \\ & + C\cosh(\Omega x) + D\sinh(\Omega x)] + ax + b \end{aligned} \tag{23}$$

with:

$$\Omega = \sqrt[4]{\frac{\lambda\omega^2}{R}} \tag{24}$$

Equations deduced from the continuity and the boundary conditions allow us to determine the scalars A, B, C, D, a and b for each section (Figure 4), which leads to a quantity of 36 unknown factors. For example, at $x = L_1$, the continuity relation of u, v and dv/dx, and the condition on N, M and $T = -dM/dx$ are:

$$\begin{aligned} & u_1(L_1) = u_{dh}(L_1), \qquad v_1(L_1) = v_{dh}(L_1), \\ & \frac{dv_1}{dx}(L_1) = \frac{dv_{dh}}{dx}(L_1) \end{aligned} \tag{25}$$

$$\begin{aligned} & u_1(L_1) = u_{dl}(L_1), \quad v_1(L_1) = v_{dl}(L_1), \\ & \frac{dv_1}{dx}(L_1) = \frac{dv_{dl}}{dx}(L_1) \end{aligned} \tag{26}$$

$$\begin{aligned} N_1(L_1) &= N_{dh}(L_1) + N_{dl}(L_1), \\ M_1(L_1) &= M_{dh}(L_1) + M_{dl}(L_1), \\ T_1(L_1) &= T_{dh}(L_1) + T_{dl}(L_1) \end{aligned} \tag{27}$$

For example, at $x = 0$, we have a free boundary condition:

$$N_1(0) = 0, \quad M_1(0) = 0, \quad T_1(0) = 0 \tag{28}$$

Thus, we obtain a linear system of 36 equations. After solving this system, we calculate the impedance Z defined by:

$$Z = \frac{V}{I} = \frac{V_d}{I} \tag{29}$$

where I is the electrical current defined by:

$$I = \iint_{\text{terminal}+} \frac{dD}{dt}ds = i\omega b\int_{L_2}^{L_2+L_p} D(x)dx \tag{30}$$

By using Equation (10) we obtain:

$$I = i\omega b(\underbrace{-G\Delta\theta_p + K\Delta u_p}_{\substack{\text{Term from} \\ \text{mechanical} \\ \text{phenomena: } T_m}} + \underbrace{L_p P V_d}_{\substack{\text{Term from} \\ \text{electrical} \\ \text{phenomena: } T_e}}) \tag{31}$$

with:

$$\begin{aligned} \Delta\theta_p &= \frac{dv_p}{dx}(L_2 + L_p) - \frac{dv_p}{dx}(L_2), \\ \Delta u_p &= u_p(L_2 + L_p) - u_p(L_2) \end{aligned} \tag{32}$$

It is important to note that $|T_e| \gg |T_m|$ but that T_e is a real and T_m is a complex because of the dissipative behaviour of materials. So, the real part of the impedance, which comes from the mechanical effects, is a good indicator of the structure's modal response.

Comparison Between Model and Experimental Results

The carbon/epoxy laminate studied is a $[45°,-45°, 90°,0°]_{2S}$. The delamination is introduced between the 11th and 12th plies. In our experiments we used PZT transducers in the form of small discs (Figure 6). They are made of a 0.15 mm thick PZT ply and a 0.2 mm thick brass ply. Material characteristics are presented in Table 1. Measurements were performed with a HP3562A analyzer. Simulation was programmed in Matlab® software on a 850 MHz processor computer. Processing time was about 4 s for 300 frequency values.

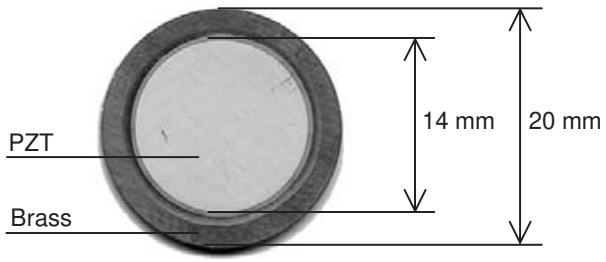

Figure 6. *PZT sensor.*

Table 2 gathers all the tests presented and commented in the following parts.

Delamination Located Inside the Beam

Figures 7 and 8 show the influence of the delamination length L_d for $L = 180\,\text{mm}$, $L_1 = 20\,\text{mm}$ and $L_2 = 23\,\text{mm}$. The impedance spectrum reveals the modes of the structure. In fact, as shown in Figure 9, some modes are located on the flaw, whereas the others are simply representative of the beam.

There is a phase shift in the impedance measurement. Therefore the real part extraction is not perfect, which explains why the real part measured is higher than the real part simulated. Consequently the resonance peaks are smaller in experimental results than in simulations.

For more clarity in the interpretation of the results, Table 3 displays the resonance frequencies extracted from Figures 7 and 8. As expected, the longer the delamination the lower the resonance frequencies. Error between simulation and experiment is about 15%. Several reasons can explain this error. First, for the intact beam, where the model is the most accurate, we can see a shift, certainly because of lack of certainty in the determination of geometric parameters and material characteristics. One can also note that the model does not take into account the shearing which is present both in the delamination ends and in the junction between the transducer and the laminate.

Table 1. Material properties.

Material Properties	Beam	Piezoelectric
Elastic properties (GPa)	$E_1/E_2/G_{12}$	E
	135/9/4	64.5
Damping coefficient (ξ)	$\xi_1/\xi_2/\xi_{11}$	0.001
$E^* = E\,(1 + i\xi)$	0.002/0.02/0.02	
Mass density (kg/m^3)	1500	7500
Permitivity ε_{22} (C/m/V)		115E 08
Coupling term d_{211} (m/V)		123E 10

Table 2. Characteristics of studied beams.

Studied Beam	L^*	L_1^*	L_d^*	L_2^*
Delamination located inside the beam	180	20	0 40 60	23
Delamination at one end of the beam	272	0	0 20 60	43
Influence of relative position between sensor and damage	180	20	40	3 23 43 63

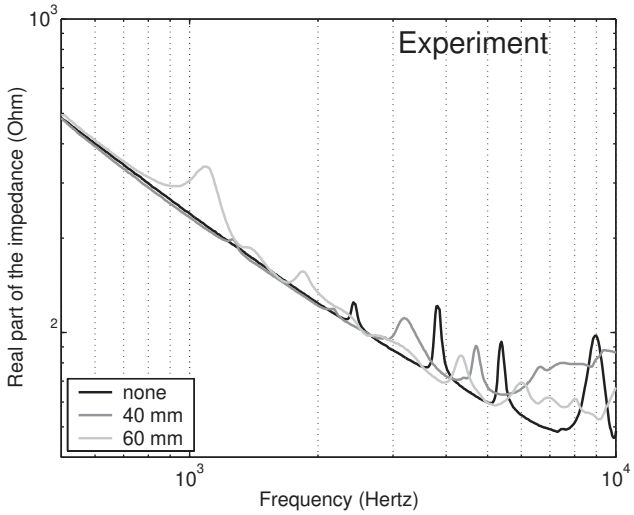

Figure 7. *Influence of delamination length L_d. Experiment. $L = 180\,\text{mm}$, $L_1 = 20\,\text{mm}$ and $L_2 = 23\,\text{mm}$.*

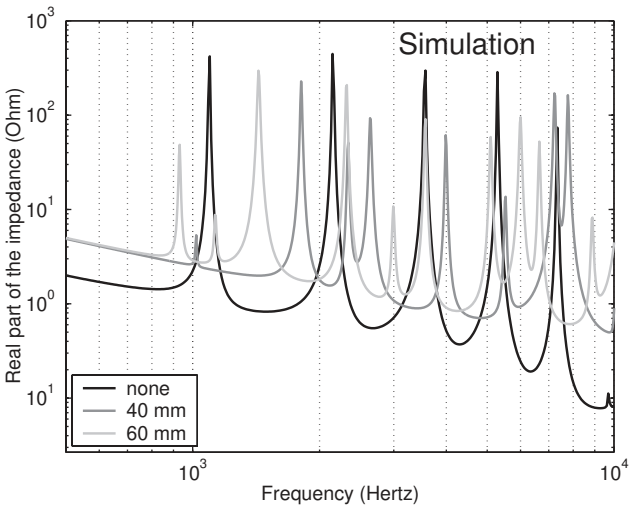

Figure 8. *Influence of delamination length L_d. Simulation. $L = 180\,\text{mm}$, $L_1 = 20\,\text{mm}$ and $L_2 = 23\,\text{mm}$.*

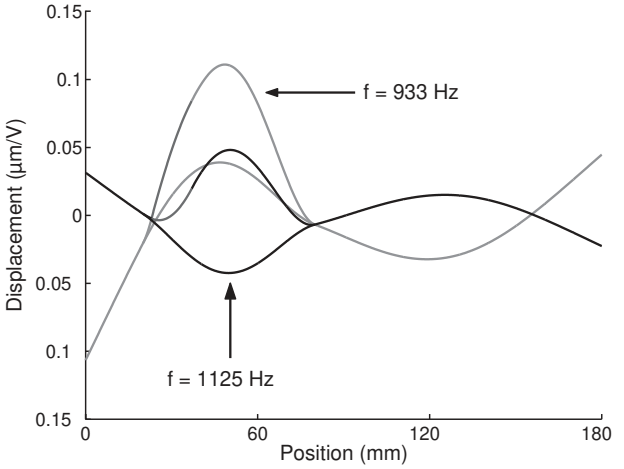

Figure 9. *Example of mode shapes for $L_d = 60\,\text{mm}$. $L = 180\,\text{mm}$, $L_1 = 20\,\text{mm}$ and $L_2 = 23\,\text{mm}$.*

Delamination at One End of the Beam

Figures 10 and 11 show the influence of the delamination length L_d for $L = 272$ mm, $L_1 = 0$ mm and $L_2 = 43$ mm. Table 4 displays resonance frequencies extracted from Figures 10 and 11. Error between simulation and experiment is lower than for previous results. When the sensor is not over the flaw, modes located on the delamination are only visible on the simulation spectrum. Nevertheless modifications appear at high frequencies, for which interpretation is more difficult.

We can also see that the general level of impedance depends on piezoelectric boundary conditions, i.e. it depends on properties of the structure near by the transducer (Vipperman, 2000). The model does not take into account the three dimensional effects which explains some relative shifts between the simulation and the experiment curves.

Influence of Relative Position Between Sensor and Damage

Identical experiments and simulations were carried out with different sensor positions for a given position and length of delamination ($L = 180$ mm, $L_1 = 20$ mm, $L_d = 40$ mm). Results are presented in Figures 12 and 13. The excitation position does not modify the modes' frequency but it influences their amplitude. It is difficult to compare experimental and simulation results for amplitudes because of the error in general level of real part. Nevertheless the resonance peaks of modes located on the delamination are less visible when the sensor is not over the flaw. The electro-mechanical impedance measurement remains a local measurement. However, as shown in the simulation, by improving the sensitivity of our measurement method we could increase the monitored zone.

Table 3. Resonance frequencies (kHz) for L 180 mm, L_1 20 mm and L_2 23 mm.

	Mode number	1	2	3	4	5	6	7	8	9	10
Experiment	Structure resonances (kHz)			2.25	3.75	5.15	7.2	8.9	10.2	12	16
$L_d = 0$	Delamination resonances (kHz)										
Simulation	Structure resonances (kHz)		1.1	2.15	3.57	5.29	7.34	9.69	12.5	15.7	19.3
$L_d = 0$	Delamination resonances (kHz)										
Experiment	Structure resonances (kHz)		1.2	2.05	3.1	4.6	7.2	8.1	9.05		
$L_d = 40$ mm	Delamination resonances (kHz)	2.85	6.4	8.9							
Simulation	Structure resonances (kHz)		1.02	1.81	2.64	4	7.22	10	12.3	15.7	18.6
$L_d = 40$ mm	Delamination resonances (kHz)	2.33	5.51	7.77	15.2	20.7					
Experiment	Structure resonances (kHz)		1.3	1.8	4.15	6.9	7.95	10.4	12		
$L_d = 60$ mm	Delamination resonances (kHz)	1.05	2.8	5.95	10.5						
Simulation	Structure resonances (kHz)		0.93	1.44	3	5.12	5.98	8.86	10.4	13.9	16.6
$L_d = 60$ mm	Delamination resonances (kHz)	1.13	2.31	3.57	6.65	11.2	15.5				

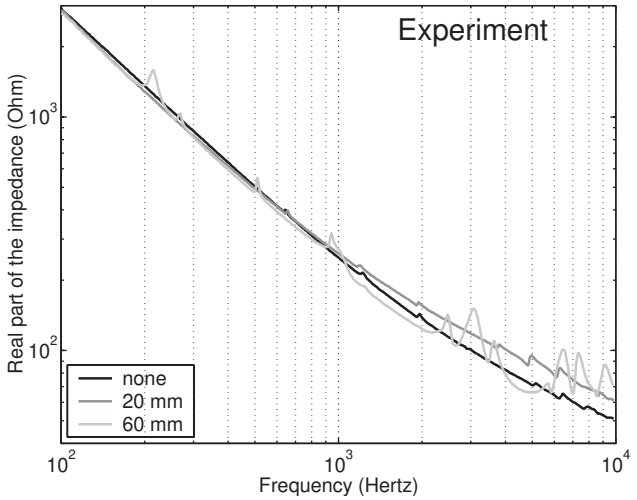

Figure 10. *Influence of delamination length L_d. Experiment. $L = 272$ mm, $L_1 = 0$ mm and $L_2 = 43$ mm.*

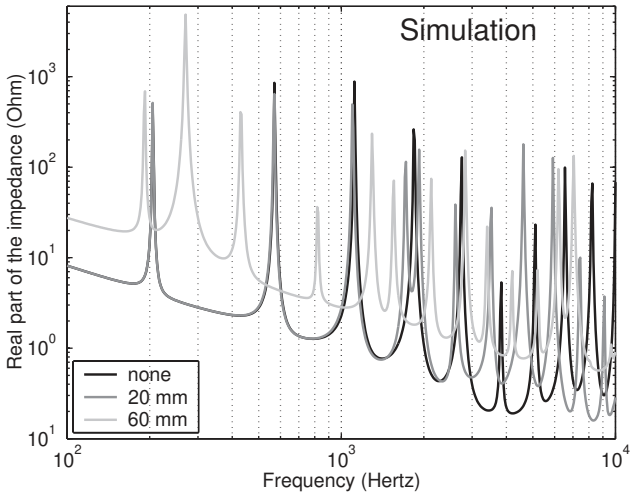

Figure 11. *Influence of delamination length L_d. Simulation. $L = 272$ mm, $L_1 = 0$ mm and $L_2 = 43$ mm.*

Table 4. Resonance frequencies (kHz) for L 272 mm, L_1 0 mm and L_2 43 mm.

	Mode Number	1	2	3	4	5	6	7	8	9	10
Experiment $L_d = 0$	Structure resonances (kHz)		0.73	1.2	1.98	3		5.1	6.3	8	
	Delamination resonances (kHz)										
Simulation $L_d = 0$	Structure resonances (kHz)	0.21	0.57	1.12	1.84	2.75	3.84	5.11	6.55	8.24	
	Delamination resonances (kHz)										
Experiment $L_d = 20$ mm	Structure resonances (kHz)		0.73	1.18	1.95		3.8	5	6.2		
	Delamination resonances (kHz)										
Simulation $L_d = 20$ mm	Structure resonances (kHz)	0.21	0.57	1.1	1.72	2.61	3.53	4.61	5.92	7.45	9.12
	Delamination resonances (kHz)	1.92									
Experiment $L_d = 60$ mm	Structure resonances (kHz)	0.21	0.505	1.21		3.05	3.6	5.7	6.4		
	Delamination resonances (kHz)	0.26	0.93	2.3		7.3					
Simulation $L_d = 60$ mm	Structure resonances (kHz)	0.19	0.43	1.29	1.56	2.83	3.4	5.2	6.19	8.05	9.64
	Delamination resonances (kHz)	0.27	0.82	2.13	4.21	7.05					

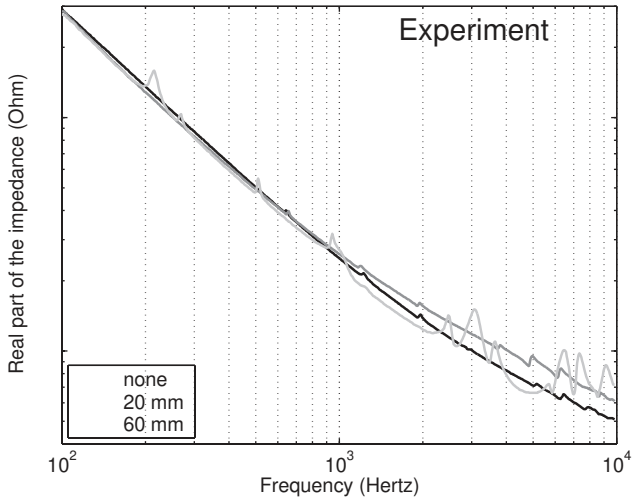

Figure 12. *Influence of piezoelectric position L_2. Experiment. $L = 180$ mm, $L_1 = 20$ mm, $L_d = 40$ mm.*

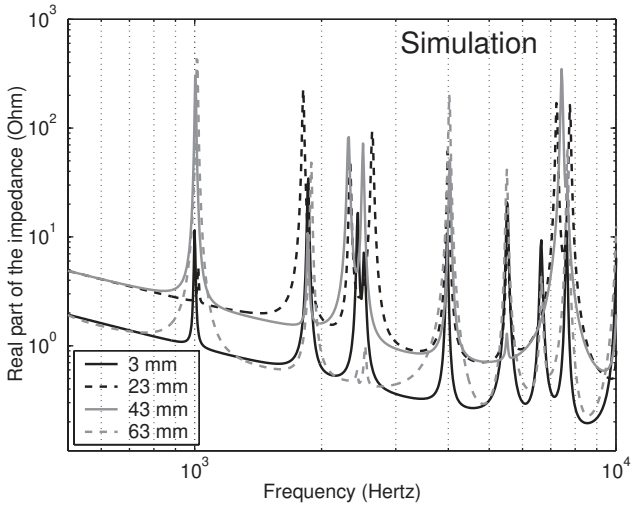

Figure 13. *Influence of piezoelectric position L_2. Simulation. $L = 180$ mm, $L_1 = 20$ mm, $L_d = 40$ mm.*

SIMULATION RESULTS

It is interesting to look at the influence of other parameters by using the model described above. In fact it is difficult and time consuming to vary the size of the transducer and the depth of the delamination during testing. For this study, we successively vary h_d, h_p and L_p, other parameters are not altered (Figure 14). To simplify the interpretation of the results, the beam is made of identical plies ($E = 42$ GPa, $\partial = \rho = 1500\,\mathrm{kg/m^3}$).

Influence of Delamination Depth

Figures 15 and 16 show the spectrum of the real part of the impedance for different values of the normalised parameter h_d/h. As expected, resonance frequencies increase when h_d increases from 0.1 to $0.5\,h$ and decrease when h_d further increases from 0.5 to $0.75\,h$. Note that between the structure with $h_d = 0.25\,h$ and that with $h_d = 0.75\,h$ only the position of the sensor is different. The higher h_d, the more important the coupling between modes located in the beam and those located in the delamination. In this case, the interpretation of results is more difficult.

Influence of Sensor Size

The use of small transducers has several advantages: sensors can be bound or inserted without decreasing the ultimate strength of the structure. The mass and the rigidity of the piezoelectric do not modify the modal response of the structure and so make it easier to interpret results. Nevertheless the transducer must be big enough to observe the mode created by the damage. Figures 17 and 18 show the influences of the thickness of the transducer and its length respectively. As expected, only resonances of modes located near the sensor, and in our case, on the delamination are shifted when the thickness or the length changes.

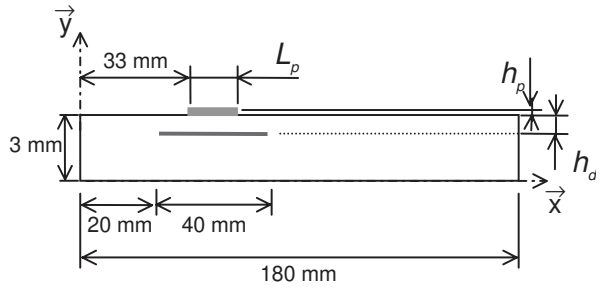

Figure 14. *Beam studied with simulations.*

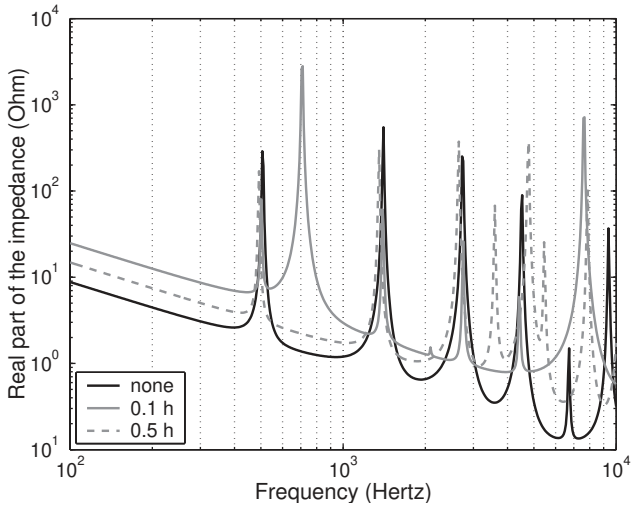

Figure 15. *Influence of delamination depth h_d. $L_p = 14\,mm$ and $h_p = 0.35\,mm$.*

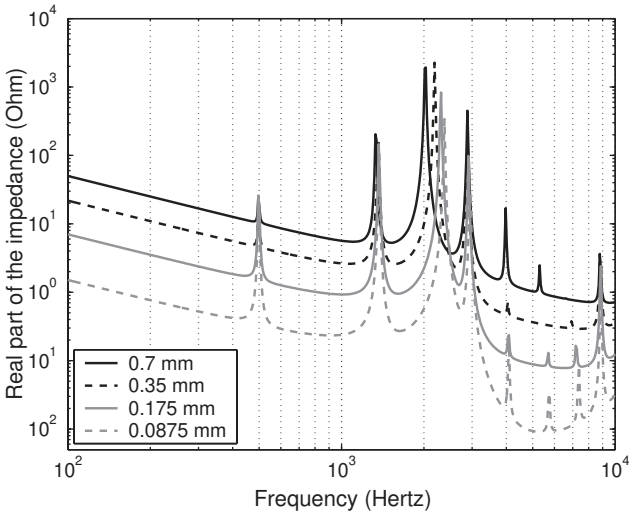

Figure 16. *Influence of delamination depth h_d. $L_p = 14\,mm$ and $h_p = 0.35\,mm$.*

This shift depends on the shape of the mode and it can be either positive or negative. When the sensor is very small, measurements gives the position of real structure resonances (without the influence of the

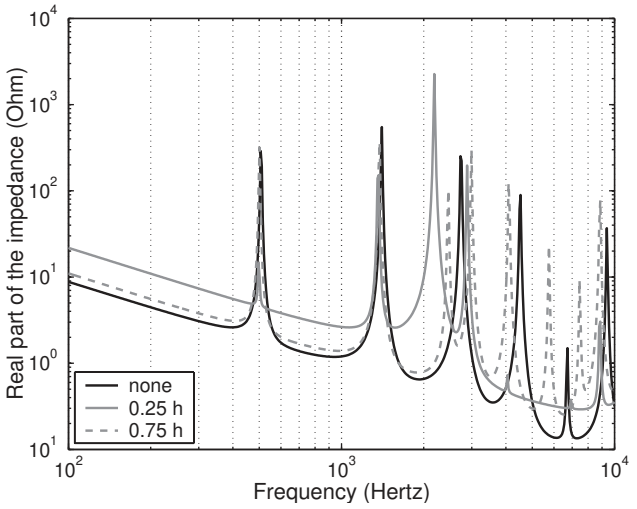

Figure 17. *Influence of sensor thickness h_p. $L_p = 14\,mm$ and $h_d = 0.75\,mm$.*

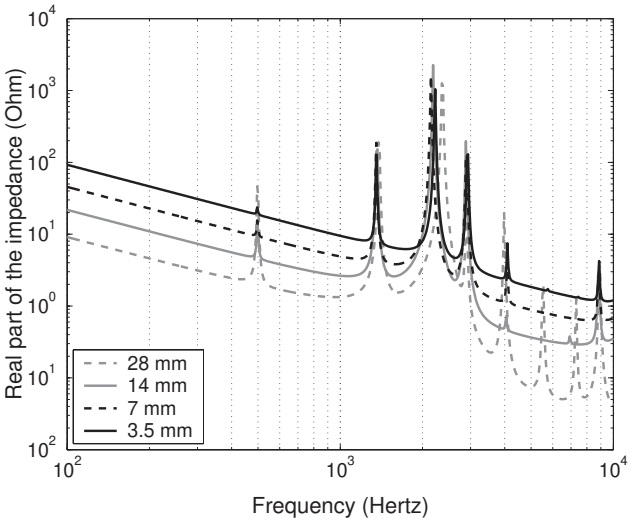

Figure 18. *Influence of sensor length L_p. $h_p = 0.35\,mm$ and $h_d = 0.75\,mm$.*

sensor). Decreasing the thickness of the transducer does not alleviate the amplitude of modes. However, decreasing its length does decrease the amplitude of modes. These results are in accordance with Equation (31). Thus, the miniaturization of sensors is made possible with a thinner piezoelectric, which is particularly convenient, if one wants to insert a transducer between two plies.

CONCLUSION

Simulation tools and experimental validation were conducted to demonstrate the feasibility of using piezoelectric sensors to detect and quantify

delamination damage in a composite laminated structure. Impedance measurement makes it possible to visualise the modes modified or created by the presence of the flaw.

A simplified and time saving model is proposed to exploit the experimental measurements. Currently, only the resonance frequencies could be used to determine, in the case of beam, the damage length by comparing experimental and simulation results. However, the modes amplitude depends on the flaw position. The measurements presented in this paper are not accurate enough to exploit this phenomenon. But, as simulations show, improving measurement will allow us to extract more of modes (low amplitude modes) and an exploitable measurement of their amplitudes. This goal can be achieved by using a synchronous demodulator with a mode locating signal processing.

Simulations show the influence of the size of the transducer and make it possible to consider the insertion of thinner sensors in composite material to generate bending modes.

The electro-mechanical impedance measurement remains a local detection method. It is adapted to monitor a critical zone or a repaired zone. Thus, we develop a long range inspection based on the Lamb wave propagation.

The next stage will consist in adapting these methods to an industrial application: monitoring delamination on the trailing edge of a helicopter blade. In addition, we have started performing experiments to measure the level of diffuse damage by impedance measurement and Lamb wave transmission.

REFERENCES

Allix, O., Leveque, D. and Perret, L. 1998. "Identification and Forecast of Delamination in Composite Laminates by an Inter laminar Interface Model," *Composites Science and Technology*, 58(5):671 678.

Giurgiutiu, V. and Rogers, C.A. 2000. "Modal Expansion Modelling of the Electro mechanical (E/M) Impedance Response of 1 D Structures," In: *Conference on System Identification and Structural Health Monitoring, Universidad Politecnica de Madrid*, Spain.

Giurgiutiu, V. and Zagrai, A.N. 2001. "Characterisation of Piezoelectric Water Active Sensors," *Journal of Intelligent Material Systems and Structures*, 11:959 976.

Keilers, C.H. and Chang, F.K. 1995. "Identifying Delamination in Composites Beams Using Built in Piezoelectrics: Part I Experiments and Analysis," *Journal of Intelligent Material Systems and Structures*, 6:649 663.

Ladevèze, P. and Le Dantec, E. 1992. "Damage Modelling of the Elementary Ply for Laminates Composites," *Composites Science and Technology*, 43(3):257 268.

Monnier, T., Jayet, Y., Guy, P. and Baboux, J.C. 2000. "The Piezoelectric Implant Method: Implementation and Pratical Applications," *Smart Materials and Structures*, 9:1 6.

Osmont, D., Barnoncel, D., Devilliers, D. and Dupont, M. 2002. "Health Monitoring of Sandwich Plates Based on the Analysis of the Interaction of Lamb Waves with Damages," In: *Proceedings of the First European Workshop on Structural Health Monitoring*, pp. 336 343.

Payan, J. and Hochard, C. 2001. "Damage Modelling of Laminated Carbon/Epoxy Composites under Static and Fatigue Loading," *International Journal of Fatigue*, 24:299 306.

Saint Pierre, N., Jayet, Y., Guy, P. and Baboux, J.C. 1998. "Ultrasonic Evaluation of Dispersive Polymers by the Piezoelectric Embedded Element Method: Modelling and Experimental Validation," *Ultrasonics*, 36:783 788.

Tracy, M. and Chang, F.K. 1998. "Identifying Impacts in Composite Plates with Piezoelectric Strain Sensors," *Journal of Intelligent Material Systems and Structures*, 9:920 928.

Vipperman, J.S. 2000. "Simultaneous Qualitative Health Monitoring and Adaptive Piezoelectric Sensoriactuation," *AIAA Journal*, 39(9):1822 1825.